无 机 化 学 学 报

2013 年　　第 29 卷　　第 3 期

目　次

论　文

CHINESE JOURNAL OF INORGANIC CHEMISTRY

Vol.29 No.3 Mar. 2013

CONTENTS

Cover

Articles

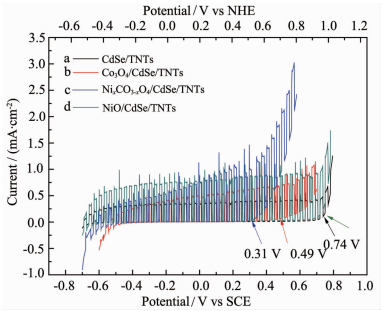

The modification of $Ni_xCo_{3-x}O_4$ can lower the overpotential of water oxidation and consequently facilitates the oxidation of water.

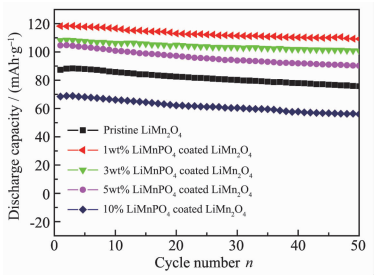

$LiMnPO_4$-coated $LiMn_2O_4$ with different contents were synthesized by hydrothermal method. The reversible capacity of the 1wt% $LiMnPO_4$ coated $LiMn_2O_4$ is 109 $mAh \cdot g^{-1}$ when cell was operated at 55 ℃ after 50 cycles. 1wt% $LiMnPO_4$ coated $LiMn_2O_4$ has excellent rate capability.

Structure and Fluorescence Property of 2D Bilayer Zn(Ⅱ) Coordination Polymer Induced by H-Bonding and π-π Interaction (English)

HU Jin-Song, LIU Xi-Hui, SHI Jian-Jun, XING Hong-Long, HE Jie

DOI:10.3969/j.issn.1001-4861.2013.00.130
Chinese J. Inorg. Chem., **2013**,**29**:444-448

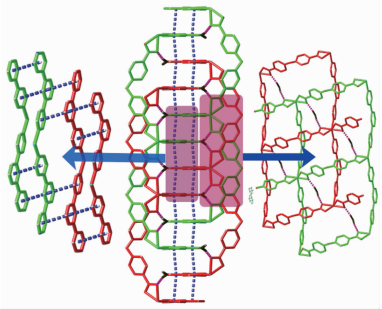

Solvothermal reaction of of 1,3-dipyridyl benzene (1,3-dpb) with 4,4′ -oxybis (benzoic acid) (H_2oba) produced a unusual bilayer 2D network by H-bonding and π-π interaction, the fluorescence property was studied.

Micro-Structure and Surface Modification of Porous Silica Coating and Their Effects on Hydrophobicity

XU Li-Li, LI Xiao-Guang, NI Xing-Yuan, SHEN Jun

DOI:10.3969/j.issn.1001-4861.2013.00.089
Chinese J. Inorg. Chem., **2013**,**29**:449-454

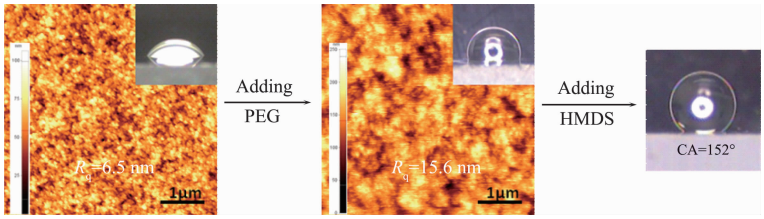

Synthesis, Structure and Comparison of Photo-electric Properties of Co(Ⅱ) Complexes with Benzoic Derivatives Li gand

JIN Jing, LIU Yong-Hua, LIU Jia-Cao, NIU Shu-Yun

DOI:10.3969/j.issn.1001-4861.2013.00.108
Chinese J. Inorg. Chem., **2013**,**29**:455-464

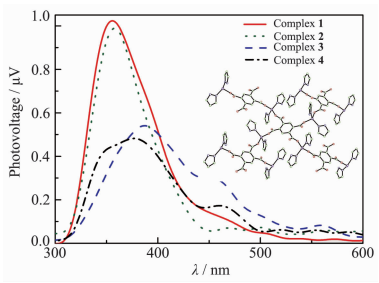

The photoelectric properties were studied by SPS. The structure of the complexes and coordination environment of the Co(Ⅱ) ions all affect the photoelectric responses.

3D-Mesoporous Zirconium Phosphonate NTAZP: Synthesis and Formaldehyde Oxidation by Its Supported Fe^{3+} Catalyst

JIA Yun-Jie, LI Ming-Lei, CUI Ji-Li, LIU Liang, WANG Run-Wei, YI Jian-Jun, XU Qing-Hong

DOI:10.3969/j.issn.1001-4861.2013.00.078
Chinese J. Inorg. Chem., **2013**,**29**:465-473

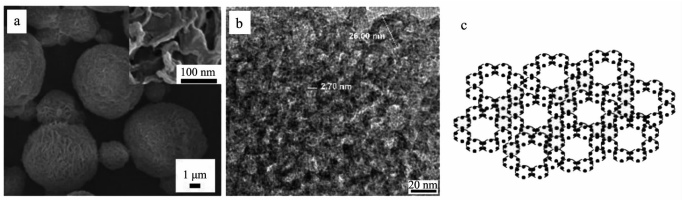

The catalytic activity for Fe^{3+}-based catalyst of NTAZP-Fe^{3+} is high for small-molecule aldehydes oxidation.

Preparation and Properties of Ag@YF_3:Eu^{3+} Core-Shell Structural Nanomaterials

LUAN Dan, SUN Ping, LIU Gui-Xia, WANG Jin-Xian, DONG Xiang-Ting, YU Wen-Sheng

DOI:10.3969/j.issn.1001-4861.2013.00.085
Chinese J. Inorg. Chem., **2013**,**29**:474-478

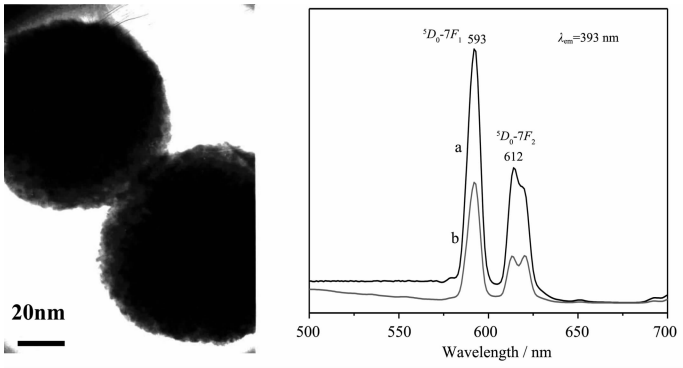

Preparation and Oil/Water Separation of Co-Ferrite/Expanded Graphite and Its Polypyrrole Composites

CHEN Hai-Feng, MA Ge, LI Liang-Chao,
WU Xi-Zhi, XIAO Qiu-Shi, XU Feng

DOI:10.3969/j.issn.1001-4861.2013.00.057
Chinese J. Inorg. Chem., **2013**,**29**:479-485

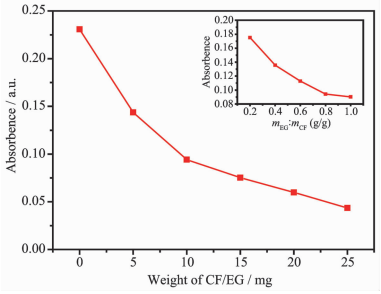

The cobalt ferrite/expanded graphite complex particles (CF/EG) were prepared by chemical co-precipitation method. The oil/water separation performance of the CF/EG complex particles was proportional to the spacing of layers in EG. The CF/EG complex particle with m_{EG}/m_{CF} ratio of 0.8 was used as a optimal material for oil/water separation due to excellently absorbing oil, easier recovery and repeated utilization.

Synthesis and Photophysical / Photochemical Properties of Aryloxy Substituted Phthalocyanine Zinc Complex

LIU Hong, ZHANG Lei, JIA Xiao,
LIU Jian-Yong, XUE Jin-Ping

DOI:10.3969/j.issn.1001-4861.2013.00.062
Chinese J. Inorg. Chem., **2013**,**29**:486-492

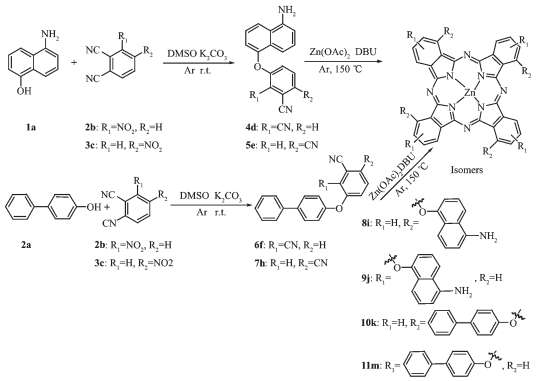

Ru-Based Catalysts Supported on Perovskite Type $BaZrO_3$ for Ammonia Synthesis

WANG Zi-Qing LIN Jian-Xin,
WANG Rong WEI Ke-Mei

DOI:10.3969/j.issn.1001-4861.2013.00.018
Chinese J. Inorg. Chem., **2013**,**29**:493-499

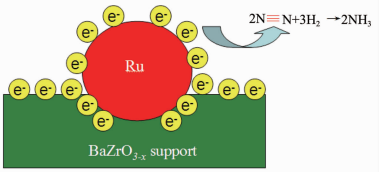

$Ru/BaZrO_3$ was an excellent catalyst for ammonia synthesis especially under the mild conditions, which was attributed to the electrons transferred from the reduced support to the Ru surface by means of the mental-support interaction.

Electrospinning Preparation and Visible-Light Photocatalytic Activity of V_2O_5 Micro-Nanorod

LUO Fei, ZHOU De-Feng, YANG Guo-Cheng,
LIU Jian-Wei, LI Zhao-Hui, MENG Jian

DOI:10.3969/j.issn.1001-4861.2013.00.104
Chinese J. Inorg. Chem., **2013**,**29**:500-506

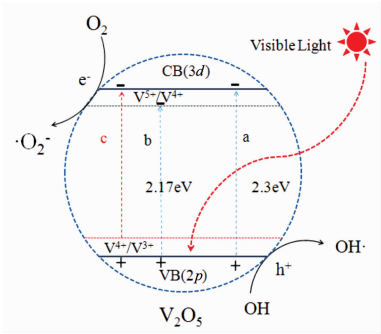

As a result of the influence of impurity energy level V^{5+}/V^{4+} and V^{4+}/V^{3+}, the V_2O_5 micro-nanorods forbidden band value diminishes, the excited electron from the value band to the conduction band transitions distance is shortened, the photocatalyst for the visible light absorption range broaden and the photocatalytic efficiency enhancement.

Influence of Dopamine on Physicochemical Properties of Calcium Phosphate Cement

LIU Zong-Guang, QU Shu-Xin,
ZHAO Jun-Sheng, LIU Yu, WENG Jie

DOI:10.3969/j.issn.1001-4861.2013.00.088
Chinese J. Inorg. Chem., **2013**,**29**:507-515

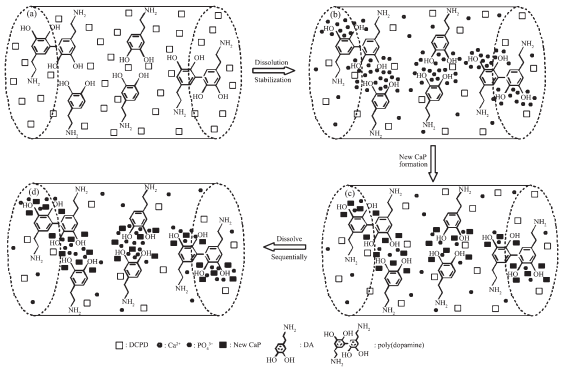

Synthesis and Crystal Structure of Eu(Ⅲ)/Dy(Ⅲ) Coordination Polymers with Benzimidazole-5,6-dicarboxylate Acid

DONG Li-Na, MA Xue, CHA Yu-E, LI Xia

DOI:10.3969/j.issn.1001-4861.2013.00.029
Chinese J. Inorg. Chem., **2013**,**29**:516-522

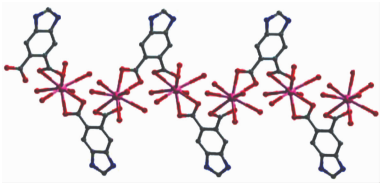

The complexes $\{[Ln(Hbidc)(bidc)(H_2O)_3]\cdot 3H_2O\}_n$ (Ln=Eu **1**, Dy **2**; H_2bidc=benzimidazole-5,6-dicarboxylic acid)have 1D chain structures by bmdc ligands and behave characteristic fluorescence of Eu^{3+} and Dy^{3+} ions, respectively.

Electronic Structure of $LiMnPO_4$ Positive-Electrode Material for Lithium-Ion Battery

ZHU Yan-Rong, XIE Ying, YI Ting-Feng,
ZENG Yuan-Yuan, ZHU Rong-Sun

DOI:10.3969/j.issn.1001-4861.2013.00.119
Chinese J. Inorg. Chem., **2013**,**29**:523-527

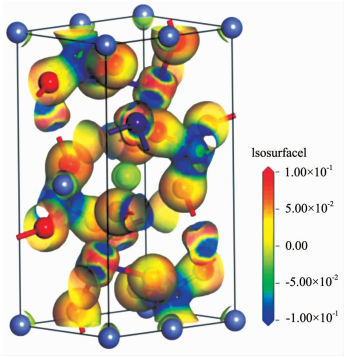

Lithium element exists in the $LiMnPO_4$ positive electrode material mainly in form of ions. There is an effective overlap between O2*p*, P3*s* orbits and Mn3*d*, O2*p* orbits, and then forms the covalent bonds.

Synthesis and Photocatalytic Activity of Mesoporous TiO_2 Using Nano-Cellulose Template Prepared by Acid Method

CHEN Xiao-Yun, LU Dong-Fang,
CHEN Yan, TAN Fei

DOI:10.3969/j.issn.1001-4861.2013.00.055
Chinese J. Inorg. Chem., **2013**,**29**:528-536

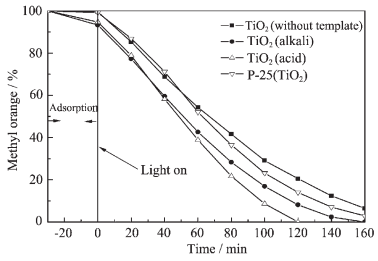

TiO_2 synthesized with nano-cellulose template exhibits mesoporous structure and high activity under UV irradiation. Hydroxyl groups of nano-cellulose and surface hydroxyl groups of TiO_2 bonding can inhibit the TiO_2 precursor growth and aggregation, and inhibit the phase transformation from anatase to rutile.

Synthesis, Crystal Structure and Properties of Novel Dicyclohexyltin Quinoline-2-Carboxylate

ZHANG Fu-Xing, WANG Jian-Qiu,
KUANG Dai-Zhi, FENG Yong-Lan,
XU Zhi-Feng, YU Jiang-Xi

DOI:10.3969/j.issn.1001-4861.2013.00.100
Chinese J. Inorg. Chem., **2013**,**29**:537-543

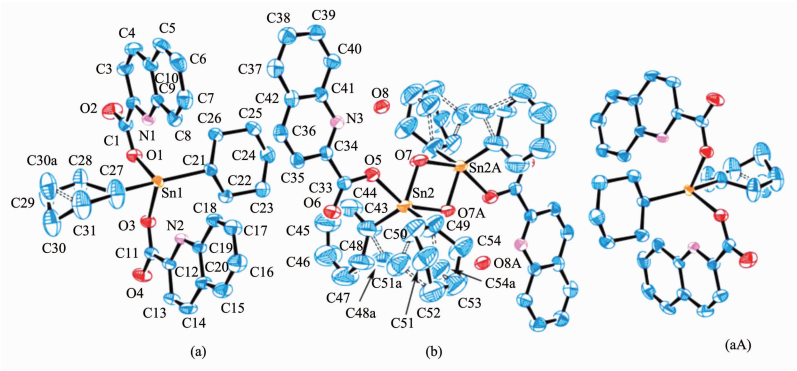

Preparation and Characterization of TiO_2 Nanotubes Array by Anodic Oxidation in Anionic Modified Glycerol-Based Electrolyte

XIAO Xiu-Feng, LIANG Jian-He,
TANG Hai-Zhen, YANG Xiao-Juan,
LIU Rong-Fang

DOI:10.3969/j.issn.1001-4861.2013.00.004
Chinese J. Inorg. Chem., **2013**,**29**:544-550

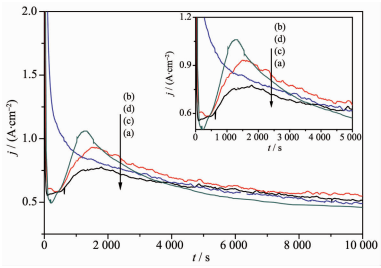

The longer TiO_2 nanotube arrays were obtained by slowing down the reduce of the anodization current and the corrosion of the F^- on the nanotube in the modified glycerol electrolyte with adding a little $NH_4H_2PO_4$ or $(NH_4)_2SO_4$ or $(NH_4)_2TiF_6$.

Influence of $ZnCl_2$ Activation on Structure and Electrochemical Performance of Carbon Aerogel Spheres

LIU Ning

DOI:10.3969/j.issn.1001-4861.2013.00.123
Chinese J. Inorg. Chem., **2013**,**29**:551-556

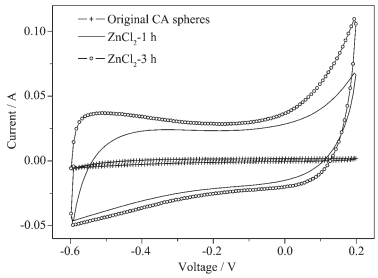

Carbon aerogel spheres were activated by zinc chloride ($ZnCl_2$), and the activated products were made into the electrodes of supercapacitor. After $ZnCl_2$ activation, the surface area and porosity of the activated products were increased, and the capacitance properties of the prepared electrodes were enhanced.

$SiO_2/TiO_{2-x}C_x/C$: Preparation, Characterization, Adsorption and Visible-Light Photocatalytic Properties

GAO Shan-Min, LIU Xin, XU Hui,
LIU Xun-Yong, HUANG Bai-Biao, DAI Ying

DOI:10.3969/j.issn.1001-4861.2013.00.120
Chinese J. Inorg. Chem., **2013**,**29**:557-564

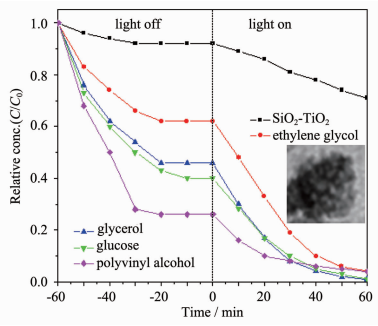

The title porous composites exhibit much higher absorption capability and better photocatalytic activity for the photooxidation of methylene blue than that of the pure silica-titania composite.

Particle Size Control for SAPO-11 Molecular Sieves

HAN Lei, CUI Xiao, LIU Xin-Mei

DOI:10.3969/j.issn.1001-4861.2013.00.103
Chinese J. Inorg. Chem., **2013**,**29**:565-570

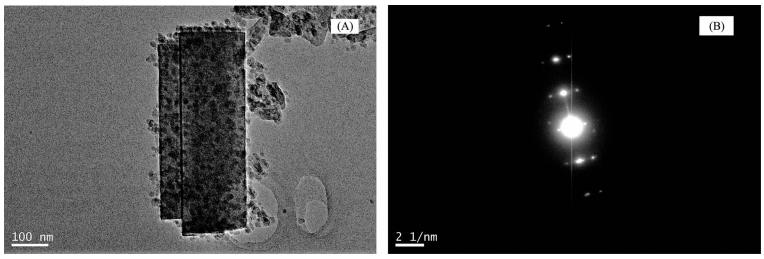

SERS of Crystal Violet Adsorbed on Submicrometer Rod-Like ZnO

MENG Wei, ZHANG Ling-Yan,
JIANG Xiao-Hong, LU Lu-De, WANG Xin

DOI:10.3969/j.issn.1001-4861.2013.00.082
Chinese J. Inorg. Chem., **2013**,**29**:571-576

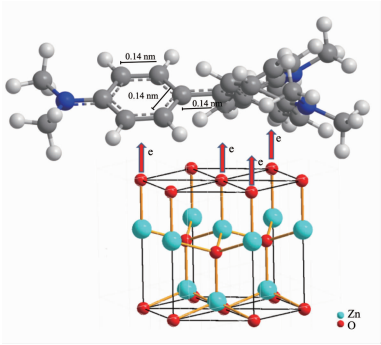

The optimized geometry of crystal violet was analyzed at the DFT/B3LYP level and the SERS enhancement factor for it adsorbed on ZnO is up to 1.2×10^2, which is attributed to chemical enhancement.

Polyethylene Glycol Stabilized RuB Nanoparticles: an Effective Catalyst for Selective Hydrogenation of Benzene to Cyclohexene

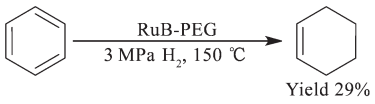

RuB nanoparticles stabilized by PEG show an effective catalytic activity and selectivity to hydrogenation of benzene to cyclohexene.

ZHANG Ye, FU Hai-Yan,
LI Rui-Xiang, CHEN Hua, LI Xian-Jun

DOI:10.3969/j.issn.1001-4861.2013.00.046
Chinese J. Inorg. Chem., **2013**,**29**:577-582

A Multi-quaternary Ammonium Induced Synthesis of Bi_2WO_6 Sheet-Like Cluster Microspheres and Photoluminescence Properties

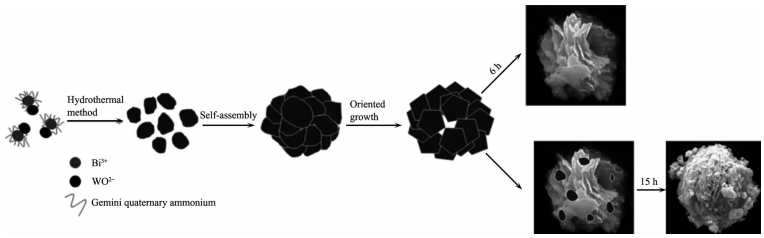

WEI Xia, ZHOU Yuan-Lin, LI Yin-Tao,
CHENG Ya-Fei

DOI:10.3969/j.issn.1001-4861.2013.00.097
Chinese J. Inorg. Chem., **2013**,**29**:583-588

Synthesis, Structure, Properties of a Two-Dimensional Manganese(Ⅱ) Coordination Polymer with α-Naphthylacetic Acid

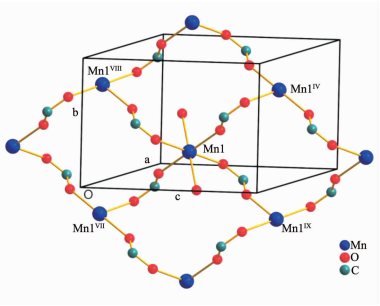

Each Mn(Ⅱ) atom is six-coordinated with a distorted octahedral geometry. The NAA^- anion acts as a μ_2-bridge linking Mn (Ⅱ) atoms generating a two-dimensional network with (4,4) topology.

YIN Fu-Jun, ZHAO Hong,
XU Xing-You, YANG Xu-Jie

DOI:10.3969/j.issn.1001-4861.2013.00.081
Chinese J. Inorg. Chem., **2013**,**29**:589-594

Bivalent and Trivalent Transition Metal Complexes of Azo Compounds Derived from Anthraquinone and Their Mutagenic-Teratogenic Effects(English)

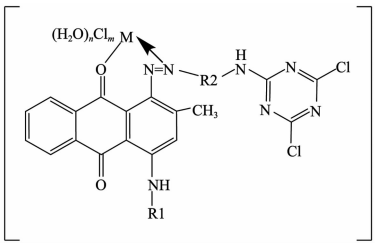

4-(5′-aminonaphtalene-3′-sulfonic acid) azo-(2″-*N*-(4‴,6‴-dichloro-*S*-triazine) benzene-5″-(β-sulfatoethyl sulfonyl)-2-methyl anthraquinone (**2a**) with $Fe^{Ⅲ}$, $Co^{Ⅱ}$ metal complexes (**2a**-Fe and **2a**-Co) in Ames/Salmonella/Microsome Test and in embryos of rats are not mutagenic and teratogenic for both TA98 and TA100 strains with and without metabolic activator S9mix.

Yildiz E, Karadeniz B, Yildiz A M,
Rencuzogullari E

DOI:10.3969/j.issn.1001-4861.2013.00.033
Chinese J. Inorg. Chem., **2013**,**29**:595-604

Hydrothermal Synthesis and Visible Light Photocatalytic Property of $Bi_{3.25}Sm_{0.75}Ti_3O_{12}$ Nanowires (English)

LIN Xue, GUAN Qing-Feng, ZOU ChunJie, LIU Ting-Ting, ZHANG Yao, LIU Chun-Bo, ZHAI Hong-Ju

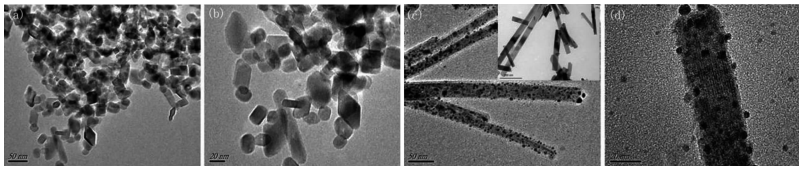

$Bi_{3.25}Sm_{0.75}Ti_3O_{12}$ (BSmT) nanowries exhibit higher photocatalytic activities in the degradation of methyl orange (MO) under visible light irradiation than that of traditional N-TiO_2 and pure $Bi_4Ti_3O_{12}$ (BIT).

DOI:10.3969/j.issn.1001-4861.2013.00.102
Chinese J. Inorg. Chem., **2013**,**29**:605-612

DNA Interaction and Antitumor Activities of Ruthenium(Ⅱ) Polypyridyl Complex (English)

XU Li, CHEN Yu, WU Jia-Huan, WEN Ban-Kang

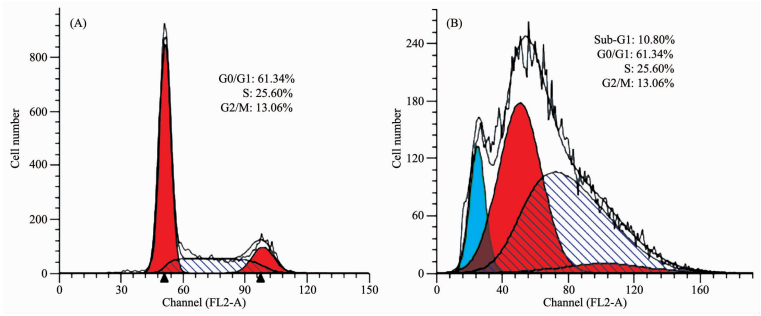

DOI:10.3969/j.issn.1001-4861.2013.00.107
Chinese J. Inorg. Chem., **2013**,**29**:613-620

Structures and Magnetic Properties of Metal Phosphonates Based on 2-(Benzoimidazol-2-yl)phenylphosphonic Acid: $[Mn(2\text{-}bppH_2)_2(H_2O)]_n$ and $[Cu(2\text{-}bppH_2)_2]\cdot xCH_3OH$ (English)

YANG Xiao-Jing, BAO Song-Song, ZHENG Li-Min

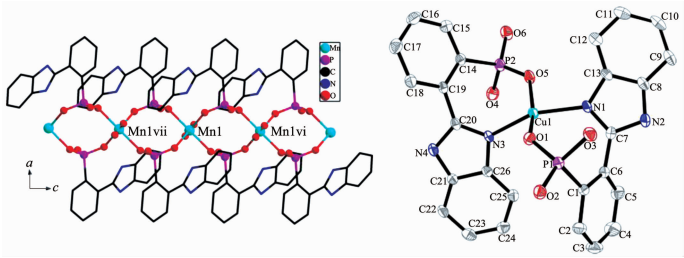

DOI:10.3969/j.issn.1001-4861.2013.00.037
Chinese J. Inorg. Chem., **2013**,**29**:621-627

Dispersion of ZnAl-LDHs Nanosheets by Cellulose to Improve Adsorption Capacity toward Phosphate (English)

ZHANG Yan-Ru, LIANG Du-Juan, WU Min, ZHAO Xin-Hua, YANG Xiao-Jing

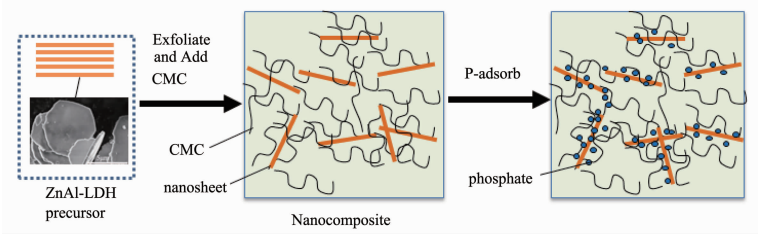

The title composite of ZnAl-LDHs nanosheets and carboxymethyl cellulose shows high selectivity toward phosphate adsorption and increases highly the phosphate-uptake amount.

DOI:10.3969/j.issn.1001-4861.2013.00.069
Chinese J. Inorg. Chem., **2013**,**29**:628-634

Biotemplating Fabrication of CdS Embedded Bionanowires at Room Temperature (English)

GONG Ya-Qiong, ZHANG He-Nan, ZHAN Huan, WEI Zeng-Yan, SU Wei

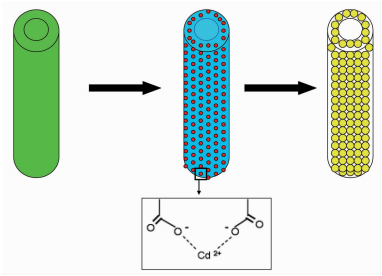

Synthesis of Cadmium Sulfide nanowires at room temperature were achieved by incubating templating bionanotubes with cadmium chloride and sodium sulfide as Cd and S precursors.

DOI:10.3969/j.issn.1001-4861.2013.00.094
Chinese J. Inorg. Chem., **2013**,**29**:635-641

Synthesis, Structure and Properties of a Porous Ni(Ⅱ) Coordination Polymer Constructed from 1,1′-(1,4-Butanediyl) bis(imidazole) and *o*-Phthalate Acid (English)

GONG Wei, NIU Qiong, NIU He-Lin, HU Lin, MAO Chang-Jie, SONG Ji-Ming, ZHANG Sheng-Yi, ZHENG Jun, CHEN Qian-Wang

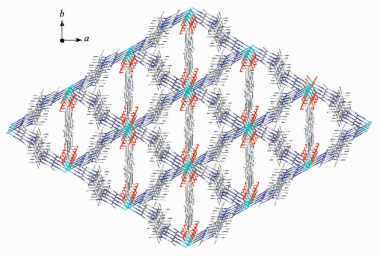

The 3-D nickel coordination polymer with triangular channels is built up of two kinds of infinite 1-D chains. It has selectivity in adsorption of N_2 and CO_2 gas and shows an overall ferromagnetic behavior.

DOI:10.3969/j.issn.1001-4861.2013.00.115
Chinese J. Inorg. Chem., **2013**,**29**:642-648

Synthesis, Crystal Structure, Thermal Stability, and Antimicrobial Activity of a Hexanuclear Iron(Ⅲ) Complex Derived from 2-[1-(2-Hydroxyethylimino)ethyl] phenol (English)

LI Hai-Hua, ZHOU Xiao-Xia, YOU Zhong-Lu

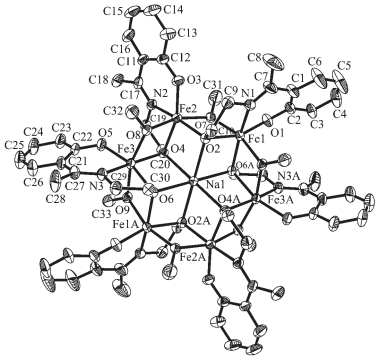

A new hexanuclear iron (Ⅲ) complex derived from 2-[1-(2-hydroxyethylimino) ethyl]phenol was prepared and structurally characterized. The thermal stability and antimicrobial activity of the complex were studied.

DOI:10.3969/j.issn.1001-4861.2013.00.080
Chinese J. Inorg. Chem., **2013**,**29**:649-653

Synthesis, Crystal Structure and Properties of the Nickel(Ⅱ) 4′-(*p*-methoxylphenyl)-2, 2′:6′,2″-terpyridine Complex

FU Wei-Wei, KUANG Dai-Zhi, ZHANG Fu-Xing, LIU Yang, LI Wei, KUANG Yun-Fei

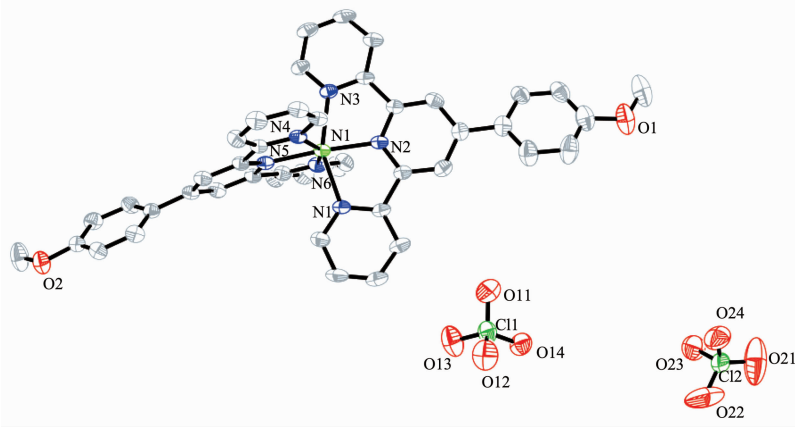

DOI:10.3969/j.issn.1001-4861.2013.00.099
Chinese J. Inorg. Chem., **2013**,**29**:654-658